Contributions of the RhoGEF activity of p210 BCR/ABL to disease progression

Share Your Story

Contributions of the RhoGEF activity of p210 BCR/ABL to disease progression

Ilona Tala, BS[1], **Ru Chen, PhD**[1], **Tinghui Hu, PhD**[1], **Ethan R Fitzpatrick, PhD**[1], **David A Williams, MD**[2], and **Ian P Whitehead, PhD**[1]

[1]New Jersey Medical School-University Hospital Cancer Center, University of Medicine and Dentistry of New Jersey, Newark, NJ 07101, USA

[2]Hematology/Oncology Division, Children's Hospital Boston and Dana-Farber Cancer Institute, Harvard Medical School, 300 Longwood Ave, Boston, MA 02115

Abstract

We have previously identified a tyrosine kinase-independent, guanine nucleotide exchange factor (GEF) activity that is contained within the region of p210 BCR/ABL that distinguishes it from p190 BCR/ABL. In the current study we have compared the transforming activity of p190 BCR/ABL, p210 BCR/ABL, and a mutant that lacks GEF activity (p210 BCR/ABL(S509A)). In cell-based, *ex vivo*, and murine bone marrow transplantation assays (BMT) the transforming activity of p210 BCR/ABL(S509A) mimics p190 BCR/ABL, and is distinct from p210 BCR/ABL. Thus, in the BMT assay, the p190 BCR/ABL and p210 BCR/ABL(S509A) transplanted mice exhibit a more rapid onset of disease than mice transplanted with p210 BCR/ABL. The reduced disease latency is associated with erythroid hyperplasia in the absence of anemia, and expansion of the MEP, CMP and GMP populations, producing a phenotype that is similar to acute myeloid leukemia (AML-M6). The disease phenotype is readily transplantable into secondary recipients. This is consistent with *ex vivo* clonogenicity assays where p210 BCR/ABL preferentially supports the growth of CFU-GM, while p190 BCR/ABL and the mutant preferentially support the growth of BFU-E. These results suggest that the GEF activity that distinguishes p210 BCR/ABL from p190 BCR/ABL actively regulates disease progression.

Keywords

Chronic myelogenous leukemia; p210 BCR/ABL; RhoGEF domain; Rho GTPase

Introduction

The Philadelphia chromosome results from a translocation that joins sequences from the BCR gene located on chromosome 22, with sequences from the ABL gene located on chromosome 9 (1, 2). Depending upon the location of the breakpoint within BCR, three different forms of the BCR/ABL fusion protein can be produced: p190 BCR/ABL, p210 BCR/ABL, and p230 BCR/ABL. Although all three fusion products are associated with leukemia, the clinical outcomes are discrete (1). p210 BCR/ABL is the most common variant and is causally associated with virtually all cases of CML; p190 BCR/ABL is found

Correspondence: Dr IP Whitehead, Cancer Center H level, New Jersey Medical School, 205 South Orange Avenue, Newark, NJ 07101, Phone: 973-972-5215, FAX: 973-972-2668, whiteip@umdnj.edu.

The authors declare no conflict of interest.

in approximately 25% of ALL; and p230 BCR/ABL has been observed in a subset of the chronic neutrophilic leukemias (3). In all cases the leukemia is dependent upon a constitutive tyrosine kinase activity that resides within the ABL sequences. Since the difference in the three BCR/ABL variants lies within the contributions from BCR, it seems likely that activities that reside within BCR may also contribute to disease progression. Consistent with this, cell- and animal-based studies have identified BCR sequences that are either required to support the tyrosine kinase activity (4–6), or are substrates for this activity (7). However, since all these activities lie within regions of BCR that are retained in all the fusion variants, they cannot account for the variant-specific disease outcome.

Residues 426-927 of BCR are of particular interest since they are contained within p210 BCR/ABL, but not p190 BCR/ABL. Whether or not the strong association of p190, and p210 BCR/ABL with ALL and CML, respectively, reflects the influence of these residues on leukemogenic activity, or simply reflects the innate tendency of hematopoeitic lineages to form specific rearrangements, remains unsettled. It is possible that these sequences may represent an inert spacer that regulates ABL-encoded tyrosine kinase activity by modulating the interaction between amino-terminal sequences of BCR and regulatory sequences within ABL(4, 8). It has been reported that p190 BCR/ABL has greater intrinsic tyrosine kinase activity than p210 BCR/ABL, although several studies suggest that this difference may be modest (9–11). Contained within residues 426-927 of BCR are tandem Dbl homology (DH) and pleckstrin homology (PH) domains that are characteristic of RhoGEF family members (12). Two recent studies indicate that this domain is active, and utilizes RhoA as a substrate in the context of p210 BCR/ABL (13, 14). p210 BCR/ABL can activate RhoA in cell-based assays, while p190 BCR/ABL cannot (15), and the introduction of mutations into the DH domain of p210 BCR/ABL that are predicted to eliminate the RhoGEF activity inhibit its ability to activate RhoA (13, 14). Whether or not this domain contributes to disease progression has not yet been determined.

The murine BMT model for CML provides an experimental system that allows direct comparisons of the disease phenotype that arises from specifically mutated versions of p210 BCR/ABL. Although p190 BCR/ABL and p210 BCR/ABL are able to induce a myeloproliferative-like disorder in this model, p190-BCR/ABL does so with a shorter latency (9, 10, 16). In the current study we compare the transforming activity of p190 BCR/ABL, p210 BCR/ABL, and a p210 BCR/ABL mutant that lacks RhoGEF activity. In both cell- and animal-based models, p190 BCR/ABL and the RhoGEF mutant of p210 BCR/ABL have virtually identical transforming activity, which is distinct from p210 BCR/ABL. Thus, whereas p210 BCR/ABL predominantly induces myeloid leukemias in the murine BMT model, p190 BCR/ABL and the mutant induce mixed myeloid/erythroid leukemias which are associated with a reduced disease latency. These results support a model in which the GEF activity that distinguishes p210 BCR/ABL from p190 BCR/ABL actively regulates disease progression by influencing lineage-specific leukemic expansion.

Materials and methods

Molecular constructs and cell culture

The MSCV-IRES-gfp (MIG) retroviral vector has been previously described (Addgene, Cambridge, MA) (17). MSCV-*bcr-abl*/p190-IRES-gfp, MSCV-*bcr-abl*/p210-IRES-gfp and MSCV-*bcr-abl*/p210(S509A)-IRES-gfp contain full-length p190 BCR/ABL, p210 BCR/ABL, and a p210 BCR/ABL RhoGEF mutant respectively (14). Phoenix-Ecotropic cells (ATCC, Manhassas, VA) were maintained in DMEM supplemented with 10% FBS (Gemini, Woodland, CA). Ba/F3 cells were cultured in RPMI supplemented with 10% FBS and IL-3-conditioned WEHI media. High titer retrovirus was generated using Phoenix-Ecotropic packaging cells as previously described (14).

Protein expression

Western blot analysis was performed as previously described (18). Antibodies used include: anti-Bcr (N20), anti-RhoA (26C4), anti-MLC2 (Fl-172) (Santa Cruz, Santa Cruz, CA); anti-phospho-MLC2(Ser19) (Cell Signaling, Danvers, MA). Affinity purification assays to measure the levels of endogenous GTP-bound RhoA were performed using Rhotekin-RBD Protein GST beads (Cytoskeleton, Denver, CO) as previously described (19).

Cell proliferation and apoptosis assays

Ba/F3 cells were infected by retroviral particles that encode MSCV-bcr-abl/p210-IRES-gfp, MSCV-bcr-abl/p210(S509A)-IRES-gfp, MSCV-bcr-abl/p190-IRES-gfp, or cognate vector. At 48 hr post-infection cells that express GFP were sorted by FACS, seeded in media with and without IL-3, and then grown for 24, 48 and 72 hr time points. For proliferation assays cells were counted using a hemacytometer. For cell cycle analysis cells were washed with PBS, fixed with ethanol for 20 minutes, then resuspended in PI-RNase solution (50μg/ml PI + 100μg/ml RNase A in PBS), incubated for another 20 minutes, and analyzed by flow cytometry. Quantification of apoptotic cells was performed using the Annexin V-Biotin Apoptosis Detection Kit according to the manufacturer's instructions (Calbiochem, La Jolla, CA). All experiments were performed on a minimum of three independent sorts.

Animals

BALB/c mice used in these studies were housed under pathogen-free conditions. All animal care, housing, and experimentation was conducted in accordance with protocols approved by the Institutional Animal Care and Use Committee of UMDNJ-New Jersey Medical School.

Bone marrow transduction

Retroviral transduction of bone marrow was done as previously described (20). Briefly, bone marrow cells were harvested and an enriched stem cell/mononuclear cell fraction was purified via Ficoll separation (Histopaque-1083; Sigma, St. Louis, MO). If cells were to be used for transplantations the mice were injected with 3.0 mg 5-Fluorouracil 6 days prior to harvesting. Prior to retroviral transduction, cells (2×10^6/ml) were prestimulated for 48 hours in IDMEM containing 10% Premium FBS (Atlanta Biologicals, Lawrenceville, GA), 2% Penicillin/Streptomycin, and 100 ng/ml each of recombinant murine TPO, G-CSF, and SCF (Peprotech, Rocky Hill, NJ). For primary transduction, cells were resuspended in appropriate retroviral supernatant containing growth factors and seeded onto fibronectin coated wells ((21); Retronectin; Takara Bio, Otsu, Japan). After 24 hours incubation, cells were resuspended in fresh retroviral supernatant and incubated for an additional 48 hours. GFP positive cells were then sorted by FACS (FACSDiVA, BD Biosciences, Franklin Lakes, NJ).

Ex vivo analysis of murine hematopoietic progenitor cells

GFP sorted primary bone marrow cells were serially diluted in triplicate in 24-well plates in Whitlock-Witte media (RPMI supplemented with 5% FBS, 200 μM L-glutamine, 50 μM 2-mercaptoethanol and penicillin-streptomycin). Cells were cultured for 3 weeks and were scored as positive for transformation when the number of cell exceeded 1×10^6 cells per ml of medium. MethoCult GF M3434 and M3630 (StemCell Technologies, Vancouver, Canada) was used to detect and quantify mouse hematopoietic progenitors in bone marrow following the manufacturer's instructions. To confirm the identity of colonies, cells were dissociated and stained with Hema 3.

Bone marrow transplantation

For bone marrow transplantations both GFP positive and negative cells were sorted by FACS (FACSDiVA, BD Biosciences, Franklin Lakes, NJ). Transplantations were performed by injecting 5.0×10^4 GFP positive cells and 3.5×10^5 GFP negative cells into the tail vein of recipient BALB/c mice that had been lethally irradiated with a split dose of 900 rads (Mark I irradiator (model 68A), J.L. Shepherd and Associates). For secondary transplantations, a total of 1×10^6 cells (5×10^5 bone marrow cells and 5×10^5 spleen cells) from diseased mice were injected into the tail veins of sublethally (450rad) irradiated BALB/c mice.

Evaluation of disease progression by flow cytometry

Mice were euthanized through CO_2 inhalation, and hematopoietic organs were harvested. Antibodies used for staining were CD11b(Mac-1)-PE, CD45R/B220-APC, CD3e-PerCP-Cy5.5, CD71-PE, Ter119-APC and CD117-PerCP-Cy5.5 (BD Biosciences, Franklin Lakes, NJ). Flow cytometry analysis was performed on a FACSCalibur using CellQuest software (BD Biosciences, Franklin Lakes, NJ).

Histopathology

Peripheral blood smears were made with blood obtained from tail-vein puncture, and staining was performed using Hema 3 solutions (Fisher Scientific, Pittsburgh, PA). Solid organs were harvested and fixed in 10% neutral buffered formalin (Sigma, St. Louis, MI) prior to paraffin sectioning. Five micron sections were then stained with hematoxylin and eosin. Complete blood cell counts were performed on heparinized blood obtained through cardiac puncture. Manual counts were conducted using a hemacytometer and automated counts were conducted by Antech Diagnostics (Lake Success, NY).

Progenitor analysis by flow cytometry

Bone marrow cells were harvested at death and stained with biotinylated antibodies specific for the following lineage markers: CD45R (B220), Cd11b, CD8a, CD4, CD3e, Ter-119, Gr-1 and IL-7Rα (eBioscience, San Diego, CA), incubated for 30 min, then washed and stained with the following additional markers: PE-Texas Red-Streptavidin, APC-Cy7-Sca-1, Brilliant Violet 421-CD117, (BioLegend, San Diego, CA), PE-CD34 and PE-Cy7-CD16/CD32 (BD Biosciences, Franklin Lakes, NJ). FACS analysis was performed using the BD LSR II flow cytometer (BD Biosciences, Franklin Lakes, NJ).

Statistics

Statistical analyses were performed using GraphPad Prism version 5.0 (GraphPad Software). Data sets in Figure 1, 2 and 4 were analyzed using one-way ANOVA, followed by Student's *t*-test. Once the statistical analysis was complete for Figure 2, the data was converted to fold activations to facilitate ease of comparison. Kaplan-Meier curves were analyzed using a Log-rank (Mantel-Cox) test.

Results

The RhoGEF activity of p210 BCR/ABL targets RhoA signaling in hematopoietic cells

We have previously shown that the RhoGEF activity of p210 BCR/ABL utilizes RhoA as a substrate in 293T cells (14). To confirm that it also utilizes RhoA as a substrate in hematopoietic cells we infected Ba/F3 cells with bicistronic retroviral vectors that encode p190 BCR/ABL, p210 BCR/ABL, or p210 BCR/ABL(S509A), along with GFP. GFP$^+$ cells were sorted and then Western blots were performed to confirm equal expression of the proteins (Figure 1A). Affinity precipitation assays for activated RhoA were then performed

(Figure 1B). Although the level of total RhoA is equivalent in all cell lines, the level of activated RhoA is significantly higher in cells expressing p210 BCR/ABL compared to vector controls. A small, but significant increase in activated RhoA is also observed in cells that express p210 BCR/ABL(S509A) but not p190 BCR/ABL. These observations suggest that although the p210 BCR/ABL(S509A) mutant is substantially impaired in its ability to activate RhoA, it may retain some residual RhoGEF activity.

Myosin light chain 2 (MLC2) is a component of myosin that is phosphorylated on Ser 19 by ROCK, the preferred effector molecule for RhoA. To confirm activation of RhoA-mediated signaling in the transduced cell lines, lysates were examined for levels of phosphorylated MLC2 (p-MLC2(Ser19)). When compared to vector transduced cells, we observe significantly elevated levels of p-MLC(Ser19) in cells that express p210 BCR/ABL, but not in those transduced with p190 BCR/ABL or p210 BCR/ABL(S509A) (Figure 1C). This is consistent with the RhoA activity assays, and suggests that the mutant is impaired in RhoA signaling in hematopoietic cells.

The RhoGEF activity of p210 BCR/ABL influences interleukin 3 (IL-3)-dependent and -independent growth in hematopoietic cells

The Ba/F3 cells that were used to analyze Rho activity were then compared for proliferation in the presence or absence of IL-3. In the presence of IL-3, cells that express p210 BCR/ABL grow significantly slower than cells that express cognate vector (Figure 1D). In contrast, cells that express p190 BCR/ABL or p210 BCR/ABL(S509A) show an equivalent 2-fold increase in growth relative to vector. In the absence of IL-3 the majority of vector transduced cells are dead by 72h (Figure 1E). As expected, the p210 BCR/ABL transduced cells are able to proliferate in the absence of IL-3 and achieve a cell density at 72h that is similar to their density in the presence of IL-3 (5×10^5 /ml vs 4×10^5/ml) (Figure 1E). Although both the p190 BCR/ABL and p210 BCR/ABL(S509A) transduced cells also proliferate in the absence of IL-3, they achieve a cell density at 72h that is significantly lower than the p210 BCR/ABL transduced cells. Thus, although all three constructs were able to confer IL-3 independent growth, p190 BCR/ABL and p210 BCR/ABL(S509A) did so to a significantly lesser degree.

Next we determined whether the difference in growth rates of the p210 BCR/ABL and p210 BCR/ABL(S509A) transduced cells in the absence of IL-3 could be attributed to a difference in their resistance to apoptosis. For this analysis we plated 5-fold more cells than the proliferation assays in order to more accurately measure apoptosis in the vector transduced cells. When compared to vector transduced cells, cells that express p210 BCR/ABL are significantly more resistant to apoptosis at 72 h (45% vs 70% annexin positive at 72h) (Figure 1F). In contrast cells that express p190 BCR/ABL and p210 BCR/ABL(S509A) undergo apoptosis at a similar frequency than cells that express vector. Thus, although both constructs can induce a higher rate of proliferation, they do not provide the survival advantage provided by p210 BCR/ABL. To confirm these observations the cells were then stained with PI and a cell cycle analysis was performed (Figure 1G). This analysis confirmed the increased proportion of cells in sub-G1 for the p190 BCR/ABL and p210 BCR/ABL(S509A) expressing cell lines, and a reduced number of cycling cells. This difference is apparent by 24 hr post-infection.

RhoGEF activity influences transformation in murine bone marrow ex vivo assays

To explore the role of the RhoGEF domain in the transformation of murine hematopietic progenitor cells, bone marrow was collected from BALB/C mice and infected with retrovirus that express p190 BCR/ABL, p210 BCR/ABL, p210 BCR/ABL(S509A), or cognate vector. Cells were then sorted for GFP expression and plated in Whitlock-Witte

media at various dilutions in triplicate. p210 BCR/ABL induced rapid outgrowth of cultures seeded with as few as 1×10^4 cells while vector expressing cells were transformation deficient (Figure 2A). The outgrowth of p190 BCR/ABL and p210 BCR/ABL(S509A) infected cells was observed only at densities of 3×10^4 or higher, and the number of days required to reach saturation at this concentration was significantly higher. To determine whether the constructs also differ in their ability to induce outgrowth of specific lineages bone marrow colony formation was assessed on media that supports growth of granulocyte-macrophage progenitors (CFU-GM) and erythroid progenitors (BFU-E) (M3434), and on media that supports growth of B cell progenitor cells (CFU-preB) (M3630). When we compared p210 BCR/ABL to vector on the M3434 media, we observed an equivalent number of BFU-E colonies (Figure 2B), but a significant increase in CFU-GM colonies on the p210 BCR/ABL plates (Figure 2C). In contrast, when we compared p190 BCR/ABL, or the p210 BCR/ABL(S509A) mutant, to vector on the same media, we observed significantly fewer CFU-GM colonies (Figure 2C) and significantly more BFU-E colonies (Figure 2B). Thus, when grown on media that supports the growth of both BFU-E and CFU-GM, p210 BCR/ABL favors CFU-GM expansion, while p190 BCR/ABL and the mutant favor BFU-E expansion. In the CFU-preB cell assay all three constructs exhibited a similar, high level of transformation (Figure 3D). To confirm the identity of the colonies induced by the constructs, cells were dissociated from randomly chosen colonies and stained with Hema 3. As expected, the BFU-E colonies are comprised of reticulocytes and nucleated red blood cells, the CFU-GM colonies are comprised of myeloid precursors, and the CFU-pre-B colonies are comprised of lymphoid precursors (Figure 2B–D, right panels).

RhoGEF activity contributes to disease progression in a bone marrow transplantation (BMT) model for CML

To examine the role of the RhoGEF domain *in vivo* we determined whether it contributes to disease progression in the murine bone marrow transplantation model for CML. Consistent with previous studies (10, 17, 22), all p210 BCR/ABL transplanted mice (3 independent experiments, n = 20 total) become moribund within 23–38 days of transplantation displaying cachexia, a decrease in activity and increased respirations (Figure 3A, Table 1). WBC counts taken at death are elevated (Table 1). An examination of peripheral blood smears prepared when the mice become moribund reveal polychromasia and extensive leukocytosis with a predominant expansion of myeloblasts and neutrophils (Figure 3B, Table 1). In contrast, mice transplanted with p190 BCR/ABL or p210 BCR/ABL(S509A) begin to exhibit signs of overt illness earlier than those transplanted with p210 BCR/ABL (within 12 days of transplantation) and the average lifespan and the range of ages at which the mice become moribund are significantly shorter (Figure 3A, Table 1). WBC counts are elevated, and outside the normal range, but 3 fold lower than p210 BCR/ABL transplanted mice at death. The peripheral blood smears prepared when the mice become moribund also reveal polychromasia, but a more limited expansion of the myeloid lineage than p210 BCR/ABL transplanted mice. In addition, large numbers of nucleated red blood cells are observed (nRBCs; Figure 3B).

All mice were subject to histologic examination. All mice had splenomegaly (Figure 3B and Table 1) at death and showed disruption of both the white and red pulp by infiltrating myeloid cells and foci of extramedullary hematopoeisis (Figure 3C). In the liver, myeloid cells infiltrated both sinusoids and portal tracts. As previously seen in other studies (10, 17, 22), large numbers of myeloid cells were present in pulmonary capillaries, together with extensive focal hemorrhage and consolidated regions. Despite the similar pathology associated with the three constructs, the organ architecture was consistently better preserved at death in mice transplanted with p190 BCR/ABL and p210 BCR/ABL(S509A), and the spleen size was consistently smaller.

Five animals for each condition that were sacrificed due to becoming moribund were also subject to immunophenotyping (Table 2). Mononuclear cells were collected from peripheral blood, spleen and bone marrow, and examined for the expression of GFP, myeloid (CD11b), T cell (CD3), and B cell (B220) markers. At death approximately 86% of WBCs from mice transplanted with p210 BCR/ABL are GFP$^+$ compared to 53% for p190 BCR/ABL and 49% for p210 BCR/ABL(S509A) (Table 1). When this is considered along with the lower WBC counts at death (Table 2), we conclude that the shortened lifespan of the p190 BCR/ABL and p210 BCR/ABL(S509A) transplanted mice cannot be simply attributed to accelerated myeloid expansion.

Staining of the mononuclear cells with myeloid and lymphoid specific markers reveals modest qualitative differences in disease phenotype. For the p210 BCR/ABL transplanted mice all animals have myeloid leukemias. The p190 BCR/ABL and p210 BCR/ABL(S509A) transplanted mice also predominantly show myeloid expansion but also, elevated levels of B and T cells are observed in the marrow and spleen. Overall the disease phenotype of p190 BCR/ABL and p210 BCR/ABL(S509A) mice are indistinguishable.

To examine the expansion of the erythroid lineage, peripheral blood was collected at death from additional mice, and CBCs were performed to determine the number of nRBCs, reticulocytes, and erythrocytes (Table 3). At death the p210 BCR/ABL transplanted mice have normal total RBC counts, but show a 3 fold increase in reticulocytes relative to vector transplanted mice, and a small increase in nRBCs. Hemoglobin and hematocrit levels are relatively normal. The p190 BCR/ABL and p210 BCR/ABL(S509A) transplanted mice also do not exhibit anemia, and have normal hemoglobin and hematocrit levels. However, they have even higher reticulocyte counts (6 fold increase), and abnormally high numbers of circulating nRBCs. To confirm the expansion of the erythroid lineage we stained the peripheral blood, bone marrow, and spleen of the mice for erythroid markers (Table 3, CD71+/Ter119+). For this analysis mature RBCs were removed with Ficoll, rather than lysis buffer, to preserve fragile nRBCs. Although all three constructs show elevated numbers of CD71$^+$/Ter119$^+$ cells relative to vector, a consistently higher number of cells is observed in the p190 BCR/ABL and p210 BCR/ABL(S509A) transplanted mice (Table 3).

The elevated numbers of blast cells observed in the blood smears suggests that the p190 BCR/ABL and p210 BCR/ABL(S509A) transplanted mice may be succumbing to more acute leukemia's than the p210 transplanted mice. To confirm this, peripheral blood, bone marrow and spleen was collected from randomly selected mice and cells were stained for CD117 (Table 4), a marker for AML. In all three tissues examined the number of GFP$^+$/ CD117$^+$ cells was slightly increased in the p210 BCR/ABL transplanted mice relative to the vector transplanted mice. In contrast, the number of GFP$^+$/CD117$^+$ cells was dramatically increased in the p190 BCR/ABL and p210 BCR/ABL(S509A) transplanted mice suggesting a more acute phenotype. In order to determine whether a particular progenitor population was selectively amplified in the p190 BCR/ABL and p210 BCR/ABL(S509A) transplanted mice, progenitor flow was performed on the bone marrow cells. Our analysis showed that GMPs, CMPs and MEPs are significantly increased in the p190 BCR/ABL and p210 BCR/ ABL(S509A) transplanted mice relative to the p210 BCR/ABL transplanted mice, but the greatest increase is observed for the MEPs (Figure 4A and 4B).

In order to confirm that the erythroid expansion observed in the p190 and mutant transplanted mice is an element of the malignancy, and not a reactive process, secondary transplantations were performed. Of the five primary tumors examined from the p210 BCR/ ABL transplanted mice two transmitted a myeloproliferative disease with a longer latency but similar phenotype (Figure 4C). The remaining three developed a B-ALL phenotype with longer disease latency. For all of the primary tumors examined for the p190 BCR/ABL and

p210 BCR/ABL(S509A) transplanted mice it was possible to transmit the erythroleukemia to the secondary recipients. Thus, in all cases the disease in the secondary recipients closely resembled the primary erythroleukemic disease, both in phenotype and latency. Collectively these observations suggest that the p190 BCR/ABL and p210 BCR/ABL(S509A) transplanted mice succumb to acute erythroid leukemia's similar to M6a in humans. They further suggest that either the MEPs have acquired self-renewal ability in the p190 BCR/ABL or mutant transplanted mice, or that the leukemia's are originating from a common progenitor population that is capable of differentiating via myeloid and erythroid lineages.

Discussion

To directly assess the contribution of RhoGEF activity to p210 BCR/ABL transformation, we have introduced a single amino acid substitution into the DH domain of p210 BCR/ABL that impairs RhoGEF activity, without affecting tyrosine kinase activity. When tested in cell, *ex vivo*, and animal-based models of transformation this mutant induces a disease phenotype that is discrete from p210 BCR/ABL, but indistinguishable from p190 BCR/ABL. When viewed in its entirety, our data suggests that the RhoGEF activity of p210 BCR/ABL directly contributes to transforming activity, and may account for the difference in disease outcome associated with p190 BCR/ABL and p210 BCR/ABL.

A comparison of transforming activity in cultured cells reveals that the RhoGEF activity may have differential effects on both proliferation and survival. Thus, in the presence of IL-3, cells that express vector, p190 BCR/ABL or the p210 BCR/ABL(S509A) mutant proliferate more rapidly than those that express p210 BCR/ABL, suggesting that the RhoGEF activity can be limiting with respect to proliferation. Interestingly, the p190 BCR/ABL and mutant expressing Ba/F3 cells do not enjoy a substantive survival advantage when IL-3 is withdrawn, which leads to a disproportionate reduction in proliferative potential relative to the p210 BCR/ABL expressing cells. Thus, the RhoGEF activity limits proliferation, but supports survival. The ability of p210 BCR/ABL to provide survival signaling has been well documented (23). Although survival is thought to be predominantly mediated by tyrosine kinase-dependent activation of the PI3K/AKT pathway, the mechanism of activation remains unsettled (23). Current evidence suggests the pathway can be activated by the GRB2/GAB2 complex which is recruited to Y177 in the BCR sequences (24), or alternatively, by recruitment and activation of CRKL and CBL (25). p210 BCR/ABL has also been shown to activate STAT5 which regulates the expression of anti-apoptotic genes such as MCL-1 and BCL-x_L (26, 27). Our current study also implicates RhoA mediated signaling pathways in p210 BCR/ABL survival signaling. RhoA signaling has been shown to promote survival in a variety of tissue types (28–31), and was recently shown to be required for the B cell activating factor-mediated survival response (32).

In the absence of Il-3 there does appear to be a limited population of p190 BCR/ABL and mutant expressing cells that can evade apoptosis and retain a high proliferative capacity. This possibility is supported by a previous study which showed that p190 BCR/ABL transformed BA/F3 cells proliferate more rapidly than p210 BCR/ABL transformed cells in the absence of IL-3 (10). In this case, the authors used cell lines that had been stably selected with neomycin, and thus would have negatively selected against cells undergoing apoptosis, and positively selected for those that retain their high proliferative potential.

Our observation that both p190 BCR/ABL and the p210 BCR/ABL(S509A) mutant are still able to drive myeloproliferation in the bone marrow transplantation model is consistent with previous studies which showed that p190 BCR/ABL induces myeloid leukemia's with reduced latency if the donor mice are pre-treated with 5-FU (9, 10). However, we observed that myeloid expansion and organ disruption at death was much more limited than in mice

transplanted with p210 BCR/ABL. Instead we observed leukocytosis, coupled with expansion of nRBCs, and reticulocytosis, suggesting that the leukemic expansion is qualitatively different. An examination of lineage specific markers and progenitor analysis confirmed the presence of elevated numbers of GMPs, CMPs and MEPs consistent with acute erythroleukemia (AML-M6) and is likely to account for the reduced disease latency associated with the transplanted mice. These tumors are readily transplantable into secondary recipients suggesting that they arise from a common progenitor population that is capable of differentiating via myeloid and erythroid lineages. Although previous studies have not noted the erythroid expansion (9, 10), these studies did not indicate that CBCs were performed, or that erythroid markers were examined. Thus, the phenotype may have been present, but not noticed.

The enhanced ability of p190 BCR/ABL and p210 BCR/ABL(S509A) to drive expansion of the erythroid lineage was further confirmed by their ability to induce BFU-Es in colony forming assays. It has been shown previously that when grown in media that allows detection of CFU-GM alone, both p190 BCR/ABL and p210 BCR/ABL support the growth of CFU-GM colonies (9). However, when we cultured bone marrow cells in the presence of media that allows detection of both BFU-E and CFU-GM, we observed that p210 BCR/ABL preferentially supports the growth of CFU-GM, while p190 BCR/ABL and the mutant preferentially support the growth of BFU-E. This suggests that the RhoGEF domain both actively supports myeloid expansion, and limits erythroid expansion. The former possibility is supported by a recent study in which an inhibitor of the RhoA/ROCK complex was shown to oppose the proliferation of human CML CD34$^+$ cells (33).

BCR/ABL rearrangements are found in 1–3% of cases of AML (including AML-M6) (34–37), and cases of erythroleukemic blast crisis have been described in CML (38). Since transition to blast crisis is generally thought to be triggered by the acquisition of secondary mutations, our results suggest that loss of Rho signaling in the leukemic stem cell that occurs secondary to p210 BCR/ABL transformation, may be sufficient to switch the fate of these cells from myeloid expansion to erythroid expansion, and account for these erythroleukemic blasts.

Acknowledgments

References

1. Melo JV. The diversity of BCR-ABL fusion proteins and their relationship to leukemia phenotype. Blood. 1996; 88:2375–2384. [PubMed: 8839828]

2. Sawyers CL. Chronic myeloid leukemia. The New England Journal of Medicine. 1999; 340:1330–1340. [PubMed: 10219069]

3. Pane F, Frigeri F, Sindona M, Luciano L, Ferrara F, Cimino R, et al. Neutrophilic-chronic myeloid leukemia: a distinct disease with a specific molecular marker (BCR/ABL with C3/A2 junction). Blood. 1996; 88:2410–2414. [PubMed: 8839830]

4. Muller AJ, Young JC, Pendergast AM, Pondel M, Landau NR, Littman DR, et al. BCR first exon sequences specifically activate the BCR/ABL tyrosine kinase oncogene of Philadelphia chromosome-positive human leukemias. Mol Cell Biol. 1991; 11:1785–1792. [PubMed: 2005881]

5. McWhirter JR, Galasso DL, Wang JY. A coiled-coil oligomerization domain of Bcr is essential for the transforming function of Bcr-Abl oncoproteins. Mol Cell Biol. 1993; 13:7587–7595. [PubMed: 8246975]

6. Maru Y, Afar DE, Witte ON, Shibuya M. The dimerization property of glutathione S-transferase partially reactivates Bcr-Abl lacking the oligomerization domain. J Biol Chem. 1996; 271:15353–15357. [PubMed: 8663064]

7. Pendergast AM, Quilliam LA, Cripe LD, Bassing CH, Dai Z, Li N, et al. BCR-ABL-induced oncogenesis is mediated by direct interaction with the SH2 domain of the GRB-2 adaptor protein. Cell. 1993; 75:175–185. [PubMed: 8402896]

8. Pendergast AM, Muller AJ, Havlik MH, Maru Y, Witte ON. BCR sequences essential for transformation by the BCR-ABL oncogene bind to the ABL SH2 regulatory domain in a nonphosphotyrosine-dependent manner. Cell. 1991; 66:161–171. [PubMed: 1712671]

9. Demehri S, O'Hare T, Eide CA, Smith CA, Tyner JW, Druker BJ, et al. The function of the pleckstrin homology domain in BCR-ABL-mediated leukemogenesis. Leukemia. 2009; 24:226–229. [PubMed: 19759561]

10. Li S, Ilaria RL Jr. Million RP, Daley GQ, Van Etten RA. The P190, P210, and P230 forms of the BCR/ABL oncogene induce a similar chronic myeloid leukemia-like syndrome in mice but have different lymphoid leukemogenic activity. The Journal of Experimental Medicine. 1999; 189:1399–1412. [PubMed: 10224280]

11. Lugo TG, Pendergast AM, Muller AJ, Witte ON. Tyrosine kinase activity and transformation potency of bcr-abl oncogene products. Science. 1990; 247:1079–1082. [PubMed: 2408149]

12. Whitehead IP, Campbell S, Rossman KL, Der CJ. Dbl family proteins. Biochim Biophys Acta. 1997; 1332:F1–23. [PubMed: 9061011]

13. Daubon T, Chasseriau J, Ali AE, Rivet J, Kitzis A, et al. Differential motility of p190bcrabl- and p210bcr-abl-expressing cells: respective roles of Vav and Bcr-Abl GEFs. Oncogene. 2008; 27:2673–2685. [PubMed: 18059343]

14. Sahay S, Pannucci NL, Mahon GM, Rodriguez PL, Megjugorac NJ, et al. The RhoGEF domain of p210 Bcr-Abl activates RhoA and is required for transformation. Oncogene. 2008; 27:2064–2071. [PubMed: 17922031]

15. Harnois T, Constantin B, Rioux A, Grenioux E, Kitzis A, et al. Differential interaction and activation of Rho family GTPases by p210bcr-abl and p190bcr-abl. Oncogene. 2003; 25(22):6445–6454. [PubMed: 14508524]

16. Kelliher M, Knott A, McLaughlin J, Witte ON, Rosenberg N. Differences in oncogenic potency but not target cell specificity distinguish the two forms of the BCR/ABL oncogene. Mol Cell Biol. 1991; 11:4710–4716. [PubMed: 1875948]

17. Pear WS, Miller JP, Xu L, Pui JC, Soffer B, et al. Efficient and rapid induction of a chronic myelogenous leukemia-like myeloproliferative disease in mice receiving P210 bcr/abltransduced bone marrow. Blood. 1998; 92:3780–3792. [PubMed: 9808572]

18. Olabisi OO, Mahon GM, Kostenko EV, Liu Z, Ozer HL, et al. Bcr interacts with components of the endosomal sorting complex required for transport-I and is required for epidermal growth factor receptor turnover. Cancer Res. 2006; 66:6250–6257. [PubMed: 16778200]

19. Korus M, Mahon GM, Cheng L, Whitehead IP. p38 MAPK-mediated activation of NF-kappaB by the RhoGEF domain of Bcr. Oncogene. 2002; 21:4601–4612. [PubMed: 12096337]

20. Thomas EK, Cancelas JA, Chae HD, Cox AD, Keller PJ, et al. Rac guanosine triphosphatases represent integrating molecular therapeutic targets for BCR-ABL-induced myeloproliferative disease. Cancer Cell. 2007; 12:467–478. [PubMed: 17996650]

21. Hanenberg H, Xiao XL, Dilloo D, Hashino K, Kato I, et al. Colocalization of retrovirus and target cells on specific fibronectin fragments increases genetic transduction of mammalian cells. Nature medicine. 1996; 2:876–882.

22. Zhang X, Ren R. Bcr-Abl efficiently induces a myeloproliferative disease and production of excess interleukin-3 and granulocyte-macrophage colony-stimulating factor in mice: a novel model for chronic myelogenous leukemia. Blood. 1998; 92:3829–3840. [PubMed: 9808576]

23. Hazlehurst LA, Bewry NN, Nair RR, Pinilla-Ibarz J. Signaling networks associated with BCR-ABL-dependent transformation. Cancer Control. 2009; 16:100–107. [PubMed: 19337196]

24. Sattler M, Mohi MG, Pride YB, Quinnan LR, Malouf NA, et al. Critical role for Gab2 in transformation by BCR/ABL. Cancer Cell. 2002; 1:479–492. [PubMed: 12124177]

25. Sattler M, Salgia R, Okuda K, Uemura N, Durstin MA, et al. The proto-oncogene product p120CBL and the adaptor proteins CRKL and c-CRK link c-ABL, p190BCR/ABL and p210BCR/ABL to the phosphatidylinositol-3' kinase pathway. Oncogene. 1996; 12:839–846. [PubMed: 8632906]

26. Gesbert F, Griffin JD. Bcr/Abl activates transcription of the Bcl-X gene through STAT5. Blood. 2000; 96:2269–2276. [PubMed: 10979976]

27. Sillaber C, Gesbert F, Frank DA, Sattler M, Griffin JD. STAT5 activation contributes to growth and viability in Bcr/Abl-transformed cells. Blood. 2000; 95:2118–2125. [PubMed: 10706883]

28. Gallagher ED, Gutowski S, Sternweis PC, Cobb MH. RhoA binds to the amino terminus of MEKK1 and regulates its kinase activity. J Biol Chem. 2004; 279:1872–1877. [PubMed: 14581471]

29. Kobayashi K, Takahashi M, Matsushita N, Miyazaki J, Koike M, et al. Survival of developing motor neurons mediated by Rho GTPase signaling pathway through Rho-kinase. J Neurosci. 2004; 24:3480–3488. [PubMed: 15071095]

30. Yoshida T, Clark MF, Stern PH. The small GTPase RhoA is crucial for MC3T3-E1 osteoblastic cell survival. Journal of Cellular Biochemistry. 2009; 106:896–902. [PubMed: 19184980]

31. Zhu S, Korzh V, Gong Z, Low BC. RhoA prevents apoptosis during zebrafish embryogenesis through activation of Mek/Erk pathway. Oncogene. 2008; 27:1580–1589. [PubMed: 17873909]

32. Zhang S, Zhou X, Lang RA, Guo F. RhoA of the Rho family small GTPases is essential for B lymphocyte development. PloS one. 7:e33773. [PubMed: 22438996]

33. Burthem J, Rees-Unwin K, Mottram R, Adams J, Lucas GS, et al. The rho-kinase inhibitors Y-27632 and fasudil act synergistically with imatinib to inhibit the expansion of ex vivo CD34(+) CML progenitor cells. Leukemia. 2007; 21:1708–1714. [PubMed: 17554385]

34. Pompetti F, Spadano A, Sau A, Mennucci A, Russo R, et al. Long-term remission in BCR/ABL-positive AML-M6 patient treated with Imatinib Mesylate. Leukemia research. 2007; 31:563–567. [PubMed: 16916543]

35. Soupir CP, Vergilio JA, Dal Cin P, Muzikansky A, Kantarjian H, et al. Philadelphia chromosome-positive acute myeloid leukemia: a rare aggressive leukemia with clinicopathologic features distinct from chronic myeloid leukemia in myeloid blast crisis. American Journal of Clinical Pathology. 2007; 127:642–650. [PubMed: 17369142]

36. Morgan GJ, Wiedemann LM, Chan LC, Price CM, Kanfer EJ, et al. A case of M-BCR-rearranged, Philadelphia-positive AML that relapsed as chronic phase CML. Blood. 1990; 75:317–318. [PubMed: 2403819]

37. Price CM, Rassool F, Shivji MK, Gow J, Tew CJ, et al. Rearrangement of the breakpoint cluster region and expression of P210 BCR-ABL in a "masked" Philadelphia chromosome-positive acute myeloid leukemia. Blood. 1988; 72:1829–1832. [PubMed: 3179449]

38. Sharma P, Dhingra KK, Roy S, Singh T. An acute myeloid leukemia M6b blast crisis with giant proerythroblasts in chronic myeloid leukemia. Journal of Pediatric Hematology/Oncology. 2009; 31:220–221. [PubMed: 19262253]
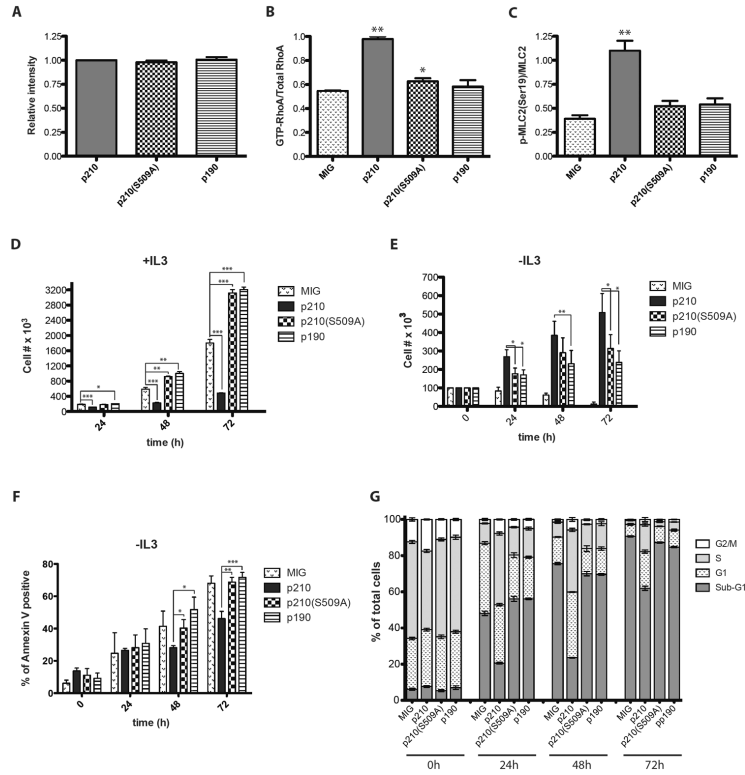
Figure 1.
The RhoGEF activity of p210 BCR/ABL regulates RhoA and influences IL-3 dependent and independent growth in hematopoietic cells. Ba/F3 cells were infected with retroviral particles that encode MSCV-bcr-abl/p210-IRES-gfp, MSCV-bcr-abl/p210(S509A)-IRES-gfp, MSCV-bcr-abl/p190-IRES-gfp, or cognate vector. (A–C) GFP-positive cells were sorted, and then plated for 48 hr. (A) Lysates were collected and examined by Western blot for expression of the Bcr-Abl constructs. (B) Lysates were also examined by affinity precipitation assays to measure levels of total (RhoA) and activated (GTP-RhoA) RhoA, and (C) by Western blot for levels of total (MLC2) and phosphorylated (p-MLC2(Ser19)) myosin light chain 2. (A–C) All Western blots were performed in triplicate and quantitated using Quantity One software (BioRad). Quantitated data shown are derived from three independent sorts, and show standard deviations, and statistical significance relative to MIG vector controls (B and C). (D–G) GFP-positive cells from the same sorts were immediately plated in the presence (D) or absence (E, F & G) of IL-3. (D&E) Cells were counted at the indicated time points. (F) The percentage of apoptotic cells was determined at the indicated time points. (G) The percentage of cells in Sub-G1, G1, S and G2/M cell cycle phases was determined at indicated time points. (A–G) Data shown are an average of three independent experiments performed on three independent sorts and show standard deviations, and statistical significance as indicated (* p < 0.05, ** p < 0.01, *** p < 0.001).
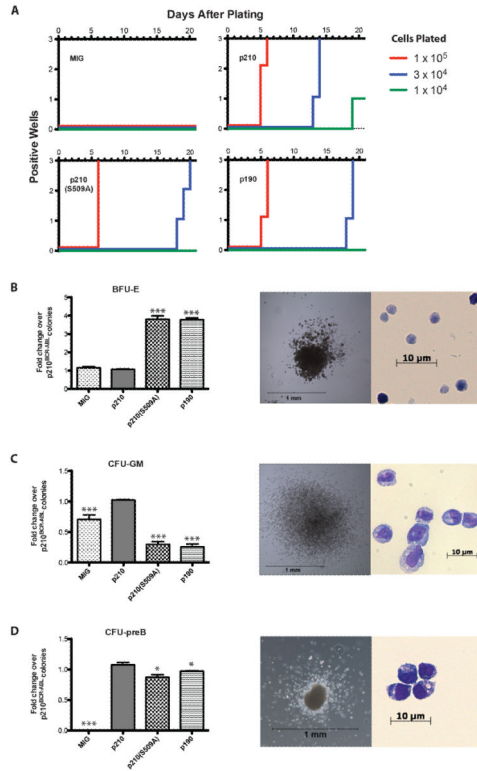
Figure 2.
Loss of RhoGEF activity alters the transforming potential of p210 BCR/ABL in murine *ex vivo* assays. Bone marrow was collected from BALB/c mice and infected with retroviral particles that encode MSCV-bcr-abl/p210-IRES-gfp, MSCV-bcr-abl/p210(S509A)-IRES-gfp, MSCV-bcr-abl/p190-IRES-gfp, or cognate vector. (A) GFP positive cells were collected and plated at the indicated cell numbers per well and in the absence of cytokines. Assays were performed in triplicate. A well was scored positive when the number of viable cells reached 10^6/well. Cell growth was monitored for 21 days. (B) GFP positive cells were collected and plated in MethoCult media that supports the growth of both BFU-E and CFU-GM (B & C), or CFU-pre-B (D). Colonies were counted and expressed as fold change relative to p210 BCR/ABL. Data shown is the average of three independent experiments and shows standard deviations, and statistical significance relative to p210 (* $p < 0.05$, ** $p < 0.01$, *** $p < 0.001$). Cells were dissociated from random colonies and stained with Hema 3 to confirm the identity of the colonies. Right panels show a representative colony and the staining of the dissociated cells. Images of colonies were visualized using an Advanced Microscopy Group microscope; EVOS (Bothell, WA, USA) at 4×PH magnification using Micron(EVOS) 2.0 software. Images of cells from colonies were visualized under oil using a Carl Zeiss microscope; Zeiss Axio Imager A1 (Thornword, NY, USA) equipped with ACHROPLAN, 100x, 1.25 numerical aperture, and acquired using AxioCam MRC camera and Axiovision 4.7.1 software.
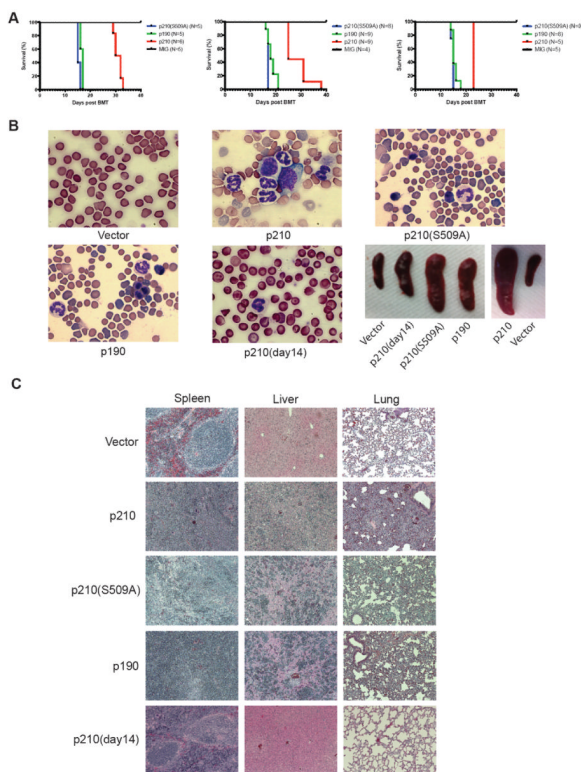
Figure 3.
Altered disease progression in mice transplanted with the p210 BCR/ABL(S509A) mutant. Bone marrow was collected from BALB/c mice and infected with retroviral particles that encode MSCV-bcr-abl/p210-IRES-gfp, MSCV-bcr-abl/p210(S509A)-IRES-gfp, MSCV-bcr-abl/p190-IRES-gfp, or cognate vector. GFP positive cells were collected and used for the bone marrow transplantation assay. (A) Survival curves for recipient mice transplanted with vector, p190 BCR/ABL, p210 BCR/ABL or p210 BCR/ABL(S509A). Kaplan-Meier curves were generated for three independent experiments. BMT = bone marrow transplantation. When comparing p210 BCR/ABL with p210 BCR/ABL(S509A), Mantel-Cox tests of the three survival curves yielded values of $p = 0.0011$ ($\chi^2 = 10.73$), $p = 0.0013$ ($\chi^2 = 10.38$) and $p < 0.0001$, ($\chi^2 = 16.35$) respectively. (B) Blood smears were performed weekly on the mice to monitor disease progression. The representative smears, and spleens, shown were taken when mice became moribund except p210 (day 14) which was done on day 14 post-BMT. Black arrows indicate nucleated red blood cells. (C) Spleen, liver, and lung tissues were also harvested at the time of death, and processed slides were stained with hematoxylin and eosin. Images of blood smears were visualized under oil using a Carl Zeiss microscope; Zeiss Axio Imager A1 (Thornword, NY, USA) equipped with ACHROPLAN, 100x, 1.25 numeical aperture, and acquired using AxioCam MRC camera and Axiovision 4.7.1 software. Images of solid organs were visualized with the same microscope using Ec Plan-NEOPLUAR 10x, 0.3 numerical aperture.
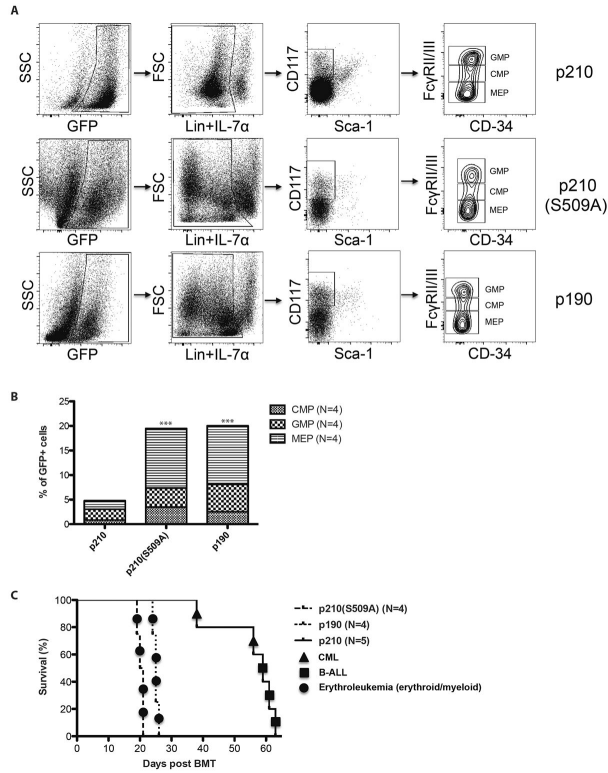
Figure 4.
The RhoGEF activity of BCR/ABL limits the self-renewal of myeloid progenitors in the BMT model. Bone marrow cells isolated from diseased mice at death were used for immunophenotypic analysis of progenitor populations. (A) Representative FACS staining profiles of progenitor populations. (B) Percentages of each progenitor populations (GMP, CMP and MEP) relative to total GFP positive cells. Values were derived from 4 mice per group, and represented as averages. Data shows statistical significance of total progenitor population relative to p210 (* $p < 0.05$, ** $p < 0.01$, *** $p < 0.001$). (C) Survival curves of secondary transplanted mice. A total of 1×10^6 cells (bone marrow and spleen) isolated from diseased mice were injected into sublethally irradiated BALB/c mice. When comparing p210 BCR/ABL with p210 BCR/ABL(S509A) a Mantel-Cox test for the survival curves yielded a value of $p = 0.004$ ($\chi^2 = 8.28$).

Table 1

Comparison of WBC counts, spleen weight, blasts and lifespan

Mouse	WBC ($10^3/\mu$l)	spleen weight (g)	% blasts	lifespan (day)
Vector[1]	5.77±0.94	0.096±0.008	0	NA
p210 BCR/ABL	118.5±31.94	0.878±0.098	26.4±5.88	28 (23–38)
p190 BCR/ABL	34.97±33.02	0.438±0.067	83.2±4.35	16 (15–21)
p210 BCR/ABL(S509A)	39.74±25.11	0.737±0.123	82.1±5.73	16 (15–17)

Data shown is for a minimum of 5 mice per group.

For lifespan, the range of ages at death is shown in parentheses.

% blasts = percentage of blasts in peripheral blood as assessed by morphology.

[1] Indicates mice that were electively sacrificed. All other mice succumbed due to disease.

Table 2

Immunophenotyping of disease progression in a BMT model for CML

Mouse (Day at death or sacrifice)	Peripheral blood % of Total Cells				Bone marrow % of Total Cells				Spleen % of Total Cells			
	%GFP+	GFP+/CD11b+	GFP+/CD3+	GFP+/B220+	%GFP+	GFP+/CD11b+	GFP+/CD3+	GFP+/B220+	%GFP+	GFP+/CD11b+	GFP+/CD3+	GFP+/B220+
Vector [1]												
#1 (Day 29)	13	4	<1	<1	17	9	<1	<1	11	3	<1	<1
#2 (Day 30)	2	<1	<1	<1	4	2	<1	<1	6	3	<1	<1
#3 (Day 30)	16	4	<1	<1	26	10	<1	<1	10	4	<1	<1
#4 (Day 32)	10	3	<1	<1	11	5	<1	<1	5	2	<1	<1
#5 (Day 32)	12	3	<1	<1	11	3	<1	<1	11	3	<1	<1
p210 BCR/ABL												
#1 (Day 29)	88	77	<1	<1	83	73	<1	<1	74	62	<1	<1
#2 (Day 32)	87	70	<1	<1	79	61	<1	<1	63	50	<1	<1
#3 (Day 30)	80	78	<1	<1	82	75	<1	<1	65	48	<1	<1
#4 (Day 32)	90	78	<1	<1	82	65	<1	<1	63	51	<1	<1
#5 (Day 30)	86	68	<1	<1	79	54	<1	<1	63	30	<1	<1
p190 BCR/ABL												
#1 (Day 16)	71	70	1	<1	56	36	7	4	43	19	10	7
#2 (Day 17)	55	53	1	1	53	35	5	5	47	16	6	8
#3 (Day 17)	46	41	3	2	45	27	6	6	29	18	5	4
#4 (Day 16)	33	32	<1	<1	40	25	5	3	34	16	5	3
#5 (Day 17)	62	57	<1	<1	50	33	10	7	41	29	9	2
p210 BCR/ABL (S509A)												
#1 (Day 16)	55	52	<1	<1	52	40	10	2	36	21	14	1
#2 (Day 15)	50	48	<1	<1	47	39	2	<1	41	36	5	<1
#3 (Day 16)	47	45	1	<1	37	25	6	4	40	19	19	2
#4 (Day 15)	51	47	4	<1	43	32	10	1	35	19	15	1
#5 (Day 15)	40	38	2	<1	37	26	10	1	35	20	14	1

[1] Vector mice were electively sacrificed. All other mice succumbed due to disease.

Table 3

Analysis of erythroid dysplasia at death

Mouse	nRBC/100 WBC	% reticulocytes	RBC (10^6/(μl)	Hemoglobin, g/dl	% hematocrit	CD71$^+$/Ter119$^+$ % of total cells
Vector[1]	0	3.81±1.9	8.75±0.26	13.92±0.44	43.9±1.57	13.33±1.52
p210 BCR/ABL	2.85±2.85	14.39±4.61	9.65±1.47	16.36±2.37	52.70±8.31	30.33±2.3
p190 BCR/ABL	222.9±154.6	24.71±8.27	8.20±0.69	13.43±1.22	43.97±4.36	71.67±5.77
p210 BCR/ABL (S509A)	145.6±140.1	28.59±6.74	9.93±0.91	14.86±1.37	47.33±4.37	73.67±4.93

Data shown is for a minimum of 5 mice per group.

nRBC = nucleated red blood cells. WBC = white blood cells. RBC = red blood cells. Total cells = total mononuclear cells analyzed.

[1] Indicates mice that were electively sacrificed. All other mice succumbed due to disease.

Table 4

Analysis of CD117 expression at death

Mouse	Peripheral blood % of Total Cells		Bone marrow % of Total Cells		Spleen % of Total Cells	
	GFP+	GFP+/CD117+	GFP+	GFP+/CD117+	GFP+	GFP+/CD117+
Vector [a]						
#1	10	<1	10	2	4	<1
#2	20	<1	9	3	5	<1
#3	5	<1	7	2	4	<1
#4	9	<1	9	2	5	<1
p210 BCR/ABL						
#1	83	2	81	3	65	7
#2	71	2	85	3	74	6
#3	71	1	81	3	53	3
#4	70	1	87	3	73	5
#5	75	2	87	4	52	4
p190 BCR/ABL						
#1	45	43	47	46	58	50
#2	48	47	36	34	63	61
#3	68	66	54	53	68	65
#4	47	43	39	36	41	39
p210 BCR/ABL (S509A)						
#1	44	43	64	62	63	59
#2	60	52	39	36	45	35
#3	41	30	45	44	37	31
#4	53	46	50	41	68	45

Total cells = total mononuclear cells analyzed. Red Blood Cell Lysis Buffer was used to remove red blood cells before analysis.

[a] Indicates mice that were electively sacrificed. All other mice succumbed due to disease.